Time Scales for Charge Equilibration of O^{q+} ($3 \leq q \leq 8$) Ions during Surface-Channeling Interactions with Au(110)

L. Folkerts
Oak Ridge National Laboratory, Oak Ridge, Tennessee 37831-6372

S. Schippers*
Oak Ridge National Laboratory, Oak Ridge, Tennessee 37831-6372
and University of Osnabrück, D-49069 Osnabrück, Germany

D. M. Zehner and F. W. Meyer
Oak Ridge National Laboratory, Oak Ridge, Tennessee 37831-6372
(Received 6 September 1994)

We report on measurements of scattered projectile angular and charge state distributions for 3.75 keV/amu O^{q+} ($3 \leq q \leq 8$) ions surface channeled along the $\langle 1\bar{1}0 \rangle$ direction of a Au(110) single crystal target. Projectile trajectory calculations indicate that the projectiles spend less than 30 fs within 2 Å of the topmost Au surface layer. Nevertheless, almost complete charge equilibration is observed in the scattered projectile charge state distributions. It is concluded that, *already at the target interface*, strong screening effects are present which make possible direct capture to the projectile L and M shells in relatively large impact parameter collisions.

PACS numbers: 34.70.+e, 79.20.Rf, 79.90.+b

One of the many interesting aspects of low energy multicharged ion-solid interactions is the very fast relaxation of the ions once they penetrate the target. Fast projectile neutralization and deexcitation has been inferred previously from measurement and analysis of projectile K Auger electron [1–3] and K x-ray [4,5] emission occurring in the bulk. While the inferences made were necessarily indirect, and involved various modeling assumptions, e.g., about electron transport to the target surface, transition energies and rates for projectiles embedded in screened media, the evolution of the projectile trajectories in the target bulk, issues related to electron background stripping, etc., they nevertheless pointed to the importance of bulk screening effects that facilitated direct capture to projectile inner shells.

In the present Letter, we present the first determination of projectile charge equilibration time scales for multicharged ion interactions occurring *at the solid surface* via the measurement of charge state distributions of projectiles scattered during grazing interactions with Au(110). de Zwart *et al.* [6] have reported measurements of scattered positive charge fractions for larger incidence angle impact of multicharged ions on polycrystalline W. They did not analyze those projectiles scattered as neutrals. Moreover, as a consequence of their larger incidence angle, significant penetration of the bulk occurred. The present measurements were performed in the specular reflection regime under surface-channeling conditions as verified by observation of characteristic angular distributions for the reflected projectiles. Under such conditions there is minimal penetration of the target surface plane, and the interaction times of the projectile with the target can be accurately determined. The measured charge state fractions of the reflected projectiles were found to be essentially independent of incident charge state, indicating that charge equilibration had occurred. Using this observation together with calculated surface interaction times, projectile inner-shell capture rates are deduced that are comparable to those inferred for bulk interactions, suggesting that strong screening is established already at the target interface. Complementary evidence for the latter is the fact that the inner-shell capture is found to occur during relatively distant encounters, as selected by the experimental specular reflection condition.

In the present experiment, 3.75 keV/amu O^{q+} ($q = 3-8$) ions, produced by the ECR ion source at the ORNL Multicharged Ion Research Facility, were grazingly incident ($\psi = 1.8°$) on a clean Au(110) surface in the $\langle 1\bar{1}0 \rangle$ direction. The incident multicharged ion beam was collimated by two 0.5-mm-diam apertures to an angular divergence of about 0.1° FWHM. The single crystal Au(110) target was mounted on an x-y-z manipulator located in a UHV chamber having a base pressure of 3×10^{-10} mbar and was prepared by cycles of sputter cleaning with 1 keV Ar^+ ions and annealing at about 700 °C. Surface cleanliness was verified using electron-induced Auger electron spectroscopy. The angular distribution (polar as well as lateral) of the scattered (reflected) projectiles was monitored using a two-dimensional position sensitive detector (PSD) having a 40-mm-diam active area, and located 560 mm from the target. The PSD was mounted on an x-y manipulator which permitted measurement of the polar scattering angle ϕ_p in the range −0.8° to +5.6°. Analysis of the primary beam, used to determine $\phi_p = 0°$, as well as its angular spread, could thus be performed. In order to avoid saturation of the PSD, the total scattered ion flux to the PSD was kept below 100 kHz.

 0031-9007/95/74(12)/2204(4)$06.00

Figure 1(a) shows the intensity distribution observed on the PSD for 3.75 keV/amu O^{8+} incident on Au(110) along the $\langle 1\bar{1}0\rangle$ direction at 1.8°. The characteristic "banana" shape of the angular distribution displayed in the figure, which disappears a few degrees away from the $\langle 1\bar{1}0\rangle$ direction, is a distinct fingerprint of surface channeling. It mirrors the "corrugation" present in the surface along the $\langle 1\bar{1}0\rangle$ direction, which is 8.15 Å wide for the known (1×2) reconstruction [7] of the Au(110) surface at room temperature.

To gain some quantitative insight into the trajectories along which the projectiles travel under the conditions of surface channeling, a Monte Carlo simulation [8] was carried out in which the equations of motion of the projectile in the periodic potential of the crystal surface were solved for an ensemble of appropriate random initial conditions. The scattering potential consisted of a superposition of individual contributions (assuming a Ziegler-Biersack-Littmark (ZBL) interaction potential [9]) from a lattice cell of 72 atoms that was progressively translated along the ion trajectory. Lattice vibrations were accounted for by employing the Debye model with an anisotropic surface Debye temperature as prescribed by Jackson [10]. Image charge acceleration effects on the incoming projectile trajectory, which lead to an increase of the scattering angle with increasing projectile charge state [11–13], were accounted for by empirical adjustment of the projectile incidence angle. These effects were small for the present projectile energies and incidence angles. Figure 1(b) shows the simulation results for the above experimental conditions. As can be seen, quite good agreement with the experimentally measured angular distribution shown in Fig. 1(a) is obtained. For the scattering conditions experimentally investigated, the simulation indicates a total trajectory length within 2 Å of the topmost Au surface layer of about 220 Å, corresponding to an interaction time of only about 25 fs. In addition, the simulation gives a maximum penetration depth of 2.2 Å, which corresponds to scattering from the bottom of the surface channels. The average minimum distance of the closest approach to any of the target atoms along a particular ion trajectory was found to be about 0.65 Å, roughly 2–3 times larger than the unscreened projectile L-shell radius.

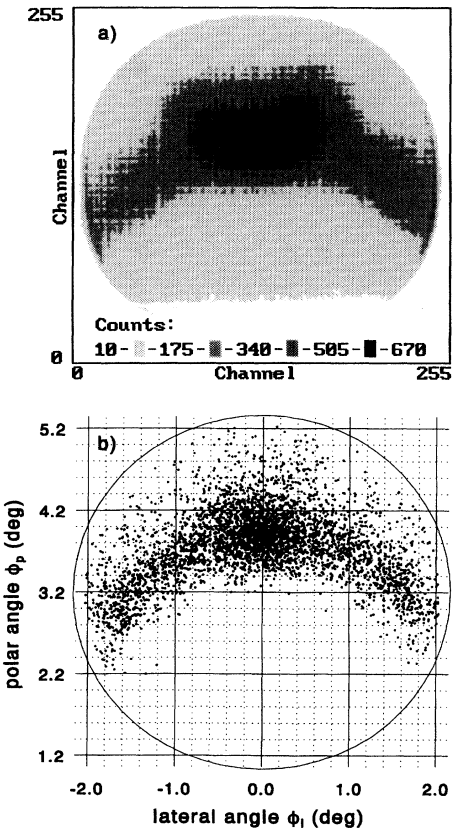

FIG. 1. Comparison of the measured (top) and simulated (bottom) scattered projectile intensity distribution on the PSD for 3.75 keV/amu O^{8+} incident on Au(110) along the $\langle 1\bar{1}0\rangle$ direction at 1.8°, showing the characteristic "banana"-shaped angular scattering distribution indicative of surface channeling.

To determine the charge state distribution of the reflected ions, a movable pair of slits located between the target and the PSD was used to select a vertical slice of the scattered beam (lateral scattering angles in range −0.15° to +0.15°). Electrostatic analysis using a pair of deflection plates immediately downstream of the slit assembly produced a series of very well resolved, horizontally displaced vertical bands, each corresponding to a particular charge state r, while the intensity distribution of each band along the vertical axis reflects its polar angular distribution. The scattered projectile charge distribution was obtained by integrating this 2D spectrum over a range of polar scattering angles ϕ_p, which for the present case was 2.0° to 4.5°. Auxiliary measurements were performed to assure that the PSD efficiency was independent of the scattered charge state.

Scattered charge state distributions were measured in this manner for oxygen ions in initial charge states down to $q = 3$, all incident at 1.8° on Au(110) at an energy of 3.75 keV/amu, and under surface-channeling conditions along the $\langle 1\bar{1}0\rangle$ direction. In Fig. 2, the fractions of final charge states r are plotted as a function of the incident charge state q. A number of remarkable features are evident in the figure. For all incident charge states investigated, the neutral fraction strongly dominates the scattered ion charge state distribution, as has been already noted by others [14]. A significant fraction of the scattered ions recedes from the surface in charge state −1 [15]. Most remarkably, the +1, 0, and −1 charge state fractions are virtually independent of initial charge state, indicating almost complete charge equilibration. As has already been found by de Zwart *et al.* [6], the scattered ion fractions of charge +2 and greater show noticeable increases when the incident ion carries one or two K vacancies. It should be noted, however, that, independent of incident charge state, the overall contribution of scattered charge states +2

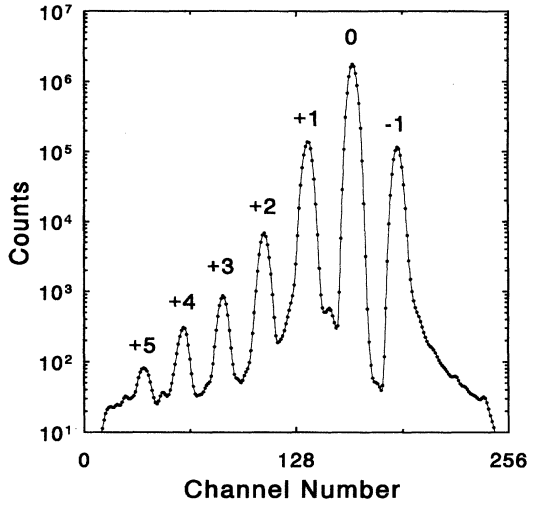

FIG. 2. Measured scattered projectile charge fractions vs initial oxygen projectile charge state for the experimental conditions of Fig. 1. Lateral scattering angle range −0.15° to +0.15°, polar scattering angle range 2.0° to 4.5°.

and higher to the total scattered ion intensity never exceeds 0.5%.

The energy dependence of the scattered charge fractions was investigated for incident O^{1+}, O^{5+}, and O^{7+} ions over the velocity range 0.064 to 0.55 a.u. The positively charged scattered ion fractions show significant increases with velocity in the investigated energy range. More interestingly, as is shown in Fig. 3, the fraction of O^- ions, with the most loosely bound electrons (E_A = 0.054 a.u.) in the ensemble of possible charge states, shows a definite velocity or energy "threshold" at v = 0.1 a.u., below which the O^- fraction is very small, and above which it steadily *increases* up to the maximum investigated velocity.

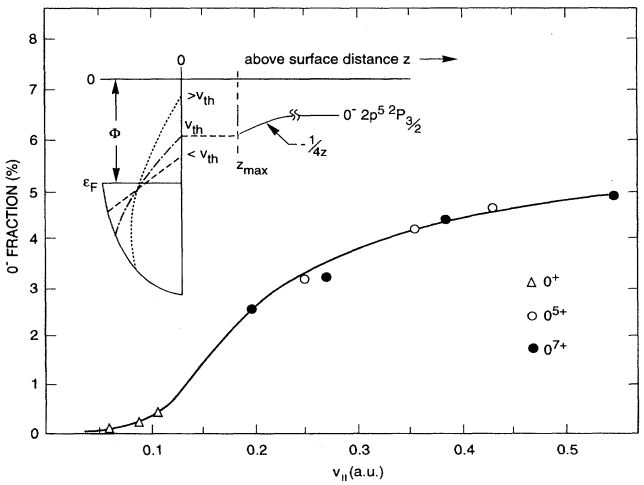

FIG. 3. O^- scattered charge fractions for O^{1+}, O^{5+}, and O^{7+} incident ions as a function of projectile velocity under the conditions of Fig. 1—the solid line is drawn to guide the eye; inset schematically indicates O^- formation mechanism.

This feature can be exploited to roughly estimate the maximum distance of negative ion formation on the receding part of the projectile trajectory. Negative ion formation velocity thresholds have been explained as arising due to "kinematic resonance" effects [16,17] in the case of projectiles having a nonzero parallel velocity component with respect to the target surface. In the projectile rest frame, the motion parallel to the surface results in an effective population of electronic states above the Fermi edge which can, at sufficiently high parallel velocities, come into resonance with weakly bound projectile electronic levels (see inset of Fig. 3). For negative ion levels, the image interaction *increases* the electron affinity with decreasing above-surface distance by $-1/4z$, where z is the distance (in a.u.) above the image plane. At the observed threshold velocity of negative ion formation, resonant capture from the top of the kinematically shifted valence band to form O^- implies a negative ion level shift (due to the image charge interaction) of –0.074 a.u., corresponding to a distance of formation above the image plane of about $3.4a_0$. This translates to a distance of 2–3 Å above the actual surface plane. Under the assumption that the O^- ion is formed by a one-electron transfer process with neutral oxygen as a necessary precursor, the observed incident charge independence of both neutral and O^- scattered ion fractions indicates that the latter distance also coincides roughly with the maximum above-surface distance at which the above noted charge equilibrium is completed.

Turning now to the question of where the charge equilibration effectively *starts* during the grazing interaction with the surface, it is recalled that resonance neutralization (RN) of the multicharged ion can already start along the approach trajectory at large distances above the surface [18], and populates high-lying Rydberg levels of the projectile (e.g., for O^{8+}, the initial n level populated is 9). Relaxation of the resulting multiexcited projectile proceeds via a time consuming autoionization cascade. Simulations of the above-surface RN and relaxation using the code developed by Burgdörfer, Lerner, and Meyer [18] were performed for charge states +7 and +8, which have the longest autoionization cascades to be traversed in order to populate the inner shells, at the perpendicular velocity corresponding to the experimental condition of Fig. 2. The feeding of the K, L, and M shells via the cascade up to the point of impact was found to be small for both ions. The other captured electrons remain in higher lying Rydberg levels, where they will be "peeled" [19] from the projectile by the increased screening it will experience upon reaching the surface. It is thus concluded that above-surface RN and relaxation along the approach trajectory do not play a significant *direct* role in the charge equilibration of these highly charged ions during their interaction with the surface.

It therefore appears that, even for the grazing collisions studied here, the dominant contribution to the charge equilibration comes from interactions occurring within roughly 2 Å of the surface. From the calculated maximum penetration depth of the trajectory simulation, we

conclude that, *for the present experimental conditions, the charge equilibration occurs within a thin slab less than 4 Å thick, which only includes the first and possibly second planes of the crystal lattice, in a time interval whose upper limit (also provided by the same trajectory simulation) is about 25 fs.*

In our earlier [1] studies of subsurface neutralization processes based on projectile K Auger electron spectroscopy, it was argued that, in the target bulk, upward shifts of the initially unfilled projectile L and M shells due to screening effects originating from the high ambient electron density, make possible direct capture and/or Auger neutralization to these inner shells [20], effectively bypassing the time consuming autoionization cascade occurring above the surface. In view of the very fast charge equilibration time inferred in the present experiment, it would appear that such a scenario may be already applicable when considering interactions with the topmost lattice plane.

Indeed, single-electron L-shell capture rates inferred from a simple phenomenological neutralization simulation are consistent with multielectron L-shell filling rates deduced earlier for conditions in which the dominant interaction was with the target bulk. The simulation [21] considers the competition between stepwise filling (via electron capture) and depletion (via ionization and, where applicable, K Auger decay) of the projectile L shell, and finds that the observed equilibrated charge distributions can be reproduced within the 25 fs surface interaction time when a 10^{15} s^{-1} single-electron L-shell capture rate is assumed, together with a 10 times slower ionization rate and previously determined K Auger rates. A more sophisticated over-the-barrier treatment developed in parallel with the present investigation by Burgdörfer [22], confirms that this high L-shell capture rate is made possible under the present experimental conditions by dynamical screening effects present *already at the target surface* which result in significant upward projectile energy shifts. By properly accounting for these effects in his calculation, he was, moreover, able to reproduce the observed scattered ion fractions, including O^- formation, without the use of fit parameters.

In conclusion, we have measured scattered charge state distributions resulting from surface-channeling interactions of 3.75 keV/amu multicharged oxygen ions with Au(110). We have shown that there is negligible direct contribution to charge equilibration at distances greater than about 2 Å above the surface, both on the incident and receding portions of the projectile trajectory. Simulations of the trajectory indicate that the projectiles spend only 20–30 fs within this distance of the surface, and that essentially no penetration of the surface occurs. Nevertheless, virtually complete charge equilibration is observed in the measured distributions. This very fast equilibration time is a strong experimental indication, that, already at the target interface (i.e., the topmost lattice plane), strong screening, essentially characteristic of the bulk, is established which facilitates direct capture to projectile inner shells.

This research was supported by the Division of Applied Plasma Physics, Office of Fusion Energy, and by the Division of Chemical Sciences, Office of Basic Energy Sciences of the U.S. Department of Energy, under Contract No. DE-AC05-84OR21400 with Martin Marietta Energy Systems, Inc. L. F. was supported through a program administered by the Oak Ridge Institute for Science and Education. S. S. gratefully acknowledges financial support by the Deutsche Forschungsgemeinschaft (DFG).

*Present address: Kernfysisch Versneller Instituut, Zernikelaan 25, 9747 AA Groningen, The Netherlands.

[1] F. W. Meyer, S. H. Overbury, C. C. Havener, P. A. Zeijlmans van Emmichoven, J. Burgdörfer, and D. M. Zehner, Phys. Rev. A **44**, 7214 (1991).
[2] J. Das, L. Folkerts, and R. Morgenstern, Phys. Rev. A **45**, 4669 (1992).
[3] R. Köhrbrück, M. Grether, A. Spieler, N. Stolterfoht, R. Page, A. Saal, and J. Bleck-Neuhaus, Phys. Rev. A **50**, 1429 (1994).
[4] H. J. Andrä *et al.*, in *ICPEAC XVII—1991, Proceedings of the International Conference on the Physics of Electron and Atomic Collisions, Brisbane, Book of Invited Papers* (Institute of Physics, Bristol, 1992), p. 89.
[5] B. D'Etat *et al.*, in *HCI—1992,* Proceedings of the Sixth International Conference on the Physics of Highly Charged Ions, AIP Conf. Proc. 274 (AIP, New York, 1992), p. 592.
[6] S. T. de Zwart, T. Fried, U. Jellen, A. L. Boers, and A. G. Drentje, J. Phys. B **18**, L623 (1985).
[7] I. K. Robinson, Phys. Rev. Lett. **50**, 1145 (1983).
[8] A. Niehof and W. Heiland, Nucl. Instrum. Methods Phys. Res., Sect. B **48**, 306 (1990).
[9] J. F. Ziegler, J. P. Biersack, and U. Littmark, in *The Stopping and Range of Ions in Solids,* edited by J. F. Ziegler (Pergamon, New York, 1985).
[10] D. P. Jackson, Surf. Sci. **43**, 432 (1974).
[11] E. Hulpke, Surf. Sci. **52**, 615 (1975).
[12] H. Winter, Europhys. Lett. **18**, 207 (1992).
[13] J. Burgdörfer and F. W. Meyer, Phys. Rev. A **47**, R20 (1993).
[14] H. Winter, C. Auth, R. Schuch, and E. Beebe, Phys. Rev. Lett. **71**, 1939 (1993).
[15] M. A. Briere *et al.*, in *ICPEAC XVIII—1993, Proceedings of the International Conference on the Physics of Electron and Atomic Collisions, Aarhus, Book of Abstracts* (Institute of Physics, Bristol, 1993), p. 774.
[16] H. Schröder and E. Kupfer, Z. Phys. A **279**, 13 (1973).
[17] J. van Wunnik, R. Brako, K. Makoshi, and D. Newns, Surf. Sci. **126**, 618 (1983).
[18] J. Burgdörfer, P. Lerner, and F. W. Meyer, Phys. Rev. A **44**, 5674 (1991).
[19] For example, F. Aumayr and H. P. Winter, Comments At. Mol. Phys. **29**, 275 (1994).
[20] L. Folkerts and R. Morgenstern, Europhys. Lett. **13**, 377 (1990).
[21] F. W. Meyer, L. Folkerts, H. O. Folkerts, and S. Schippers, HCI—1994 [Nucl. Instrum. Methods Phys. Res., Sect. B (to be published)].
[22] J. Burgdörfer, C. Reinhold, and F. W. Meyer, in Ref. [21].

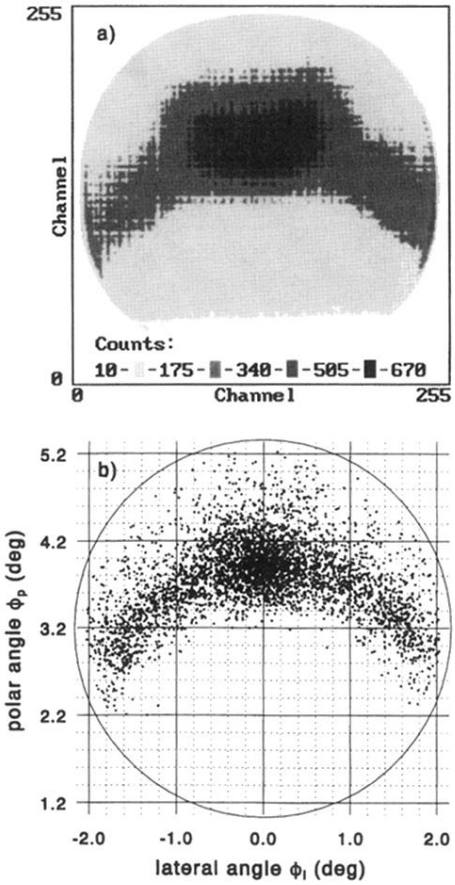

FIG. 1. Comparison of the measured (top) and simulated (bottom) scattered projectile intensity distribution on the PSD for 3.75 keV/amu O^{8+} incident on Au(110) along the $\langle 1\bar{1}0 \rangle$ direction at 1.8°, showing the characteristic "banana"-shaped angular scattering distribution indicative of surface channeling.